Computation of Rotor Blade Flows Using the Euler Equations

B. E. Wake,* N. L. Sankar,† and S. G. Lekoudis†
Georgia Institute of Technology, Atlanta, Georgia

The Euler equations are used to compute steady and unsteady three-dimensional transonic flows around nonlifting rotor blades. A hybrid numerical procedure is used that treats the spanwise derivatives explicitly and the other spatial derivatives implicitly. The steady-state results are in excellent agreement with results obtained from the full potential equation. The results for unsteady flow compare well with measurements. These results demonstrate the ability of the Euler solver to compute transonic flow around helicopter blades.

I. Introduction

THE prediction of high-speed flows around helicopter blades is of crucial importance in the development of new rotors and in the efforts to increase the forward flight speed of helicopters. Moreover, such a prediction is useful in the aeroacoustic tailoring of blade tips, so that the noise level emitted from the blade is controlled. Although the speed of helicopters is subsonic, the outboard section of the advancing blades experiences transonic flow.

The earliest attempts to compute such flows involve the use of the transonic small disturbance (TSD) equation.[1-4] Currently, the method is well developed and it provides an economical way of computing such flows. Both steady and unsteady calculations have been performed using this method. Subsequent attempts were based on the steady full potential equation.[5-10] This formulation has the capability of handling thick blades, provided the unsteady effects are not important. Recently, solutions of the unsteady full potential equation appeared in the literature.[11-13] These latest methods will undoubtedly be very useful in practice because they represent the most complete model for computing high-speed potential flows around rotor blades. Moreover, they do require smaller computer resources than the Euler and Navier-Stokes solvers.

Thus, we arrive at the category of solvers that the present work addresses. They use the Euler equations and a few papers have already appeared in the literature.[14-16] The Euler equations do not need the potential flow assumption; they admit solutions with vorticity. As a result, strong shocks can be computed. However, such solvers require an order of magnitude and more computer time than the solvers that use the potential flow assumption. Therefore, they are somewhat removed from the engineering practice for the time being. Yet, as the need for more accurate solutions that include vorticity increases and as vector computers become more available to engineers, more advanced models will find their way into the engineering practice as has happened in the past.

This paper presents calculations that are based on the method described in Ref. 15. The unsteady Euler equations are solved using a hybrid numerical procedure. The procedure advances the solution in a time accurate manner, by treating the spanwise derivatives explicitly and the other space derivatives with an alternating direction implicit procedure. The next section of the paper includes the analytical and the numerical formulation and the final section contains the discussion of the results.

Presented as Paper 85-5010 at the AIAA 3rd Applied Aerodynamics Conference, Colorado Springs, CO, Oct. 14-16, 1985; received Dec. 6, 1985; revision received Feb. 28, 1986.

*Graduate Fellow, School of Aerospace Engineering. Student Member AIAA.

†Associate Professor, School of Aerospace Engineering. Member AIAA.

II. The Analytical and the Numerical Formulation

As mentioned in the Introduction, the present study is based on the solution technique described in Ref. 15. For the sake of completeness, we repeat the procedure in the following paragraphs.

The three-dimensional Euler equations for unsteady flow can be written in conservation form as follows

$$q_t + F_x + G_y + H_z = 0 \tag{1}$$

where q is the vector containing the flow properties

$$q = \{\rho, \rho u, \rho v, \rho w, e\}^T \tag{2}$$

and F, G, H are the flux vectors given by

$$F = \begin{bmatrix} \rho u \\ \rho u^2 + p \\ \rho v \\ \rho uw \\ u(e+p) \end{bmatrix} \quad G = \begin{bmatrix} \rho v \\ \rho uv \\ \rho v^2 + p \\ \rho uw \\ v(e+p) \end{bmatrix} \quad H = \begin{bmatrix} \rho w \\ \rho uw \\ \rho vw \\ \rho w^2 + p \\ w(e+p) \end{bmatrix} \tag{3}$$

The quantity ρ is the flow density, u, v, w the Cartesian velocity components, p the pressure, and e the total energy per unit volume.

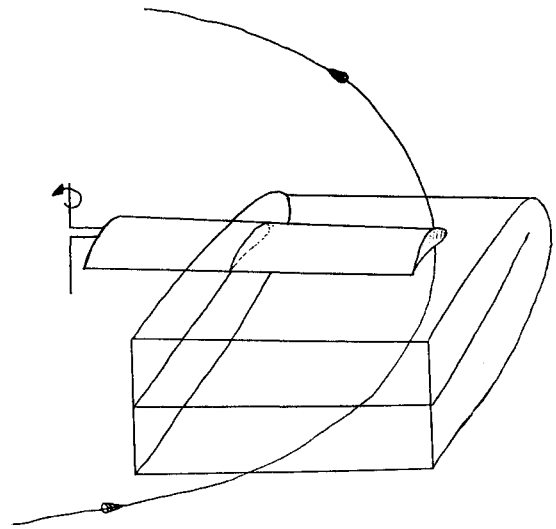

Fig. 1 Schematic diagram of computational domain.

In order to handle arbitrary rotor shapes undergoing arbitrary motions, the present calculations are performed in a computational space ξ, η, ζ, τ related to the physical space (x, y,z,t) through the following arbitrary one-to-one transformation

$$\xi=\xi(x,y,z,t)$$
$$\eta=\eta(x,y,z,t)$$
$$\zeta=\zeta(x,y,z,t)$$
$$\tau=t \tag{4}$$

In the transformed space the Euler equations may be written in the following strong conservation form

$$\hat{q}_\tau+\hat{F}_\xi+G_\eta+\hat{H}_\zeta=0 \tag{5}$$

where the quantities $\hat{q}$, $\hat{F}$, $\hat{G}$, and $\hat{H}$ are given by

$$\hat{q}=q/J$$
$$\hat{F}=(\xi_t q+\xi_x F+\xi_y G+\xi_z H)/J$$
$$\hat{G}=(\eta_t q+\eta_x F+\eta_y G+\eta_z H)/J$$
$$\hat{H}=(\zeta_t q+\zeta_x F+\zeta_y G+\zeta_z H)/J \tag{6}$$

and J is the Jacobian of the transformation.[15] As the grid points move in space, they retain their coordinate values, therefore,

$$\xi_t=-x_\tau\xi_x-y_\tau\xi_y-z_\tau\xi_z$$
$$\eta_t=-x_\tau y_x-y_\tau\eta_y-z_\tau\eta_z$$
$$\zeta_t=-x_\tau\zeta_x-y_\tau\zeta_y-z_\tau\zeta_z \tag{7}$$

The quantities η_x, η_y, etc., are the metrics of the transformation, and they are related to ξ_x, ξ_y, etc., as shown in Ref. 15. Notice that x_τ, y_τ, z_τ are the velocities of the grid points *in the inertial* coordinate system.

A body fitted coordinate system is used and a schematic outline is shown in Fig. 1. A sheared parabolic C-grid is used for the calculations and details about it can be found in Ref. 15. The unknown in the above system of equations is the flow property vector q. The time derivative of q was discretized using two point backward differences. The spatial derivatives along the ξ and the ζ directions were discretized using central differences. The quantities F and H are nonlinear functions of q at the time level $n+1$. These functions were first linearized about the time level n as follows:

$$\hat{F}^{n+1}=\hat{F}^n+\frac{\partial\hat{F}}{\partial\hat{q}}\Delta q^{n+1}$$
$$\hat{H}^{n+1}=\hat{H}^n+\frac{\partial\hat{H}}{\partial\hat{q}}\Delta q^{n+1} \tag{8}$$

The spanwise derivative $\hat{G}$ was written as a combination of the n and $n+1$ time levels. During the odd time steps, calculations were done one span station at a time, from the wing root to the outboard span station, using the latest values of the flow vector at the $n+1$ time level as soon as they are available. Thus, the quantity $\hat{G}_\eta$ was written as

$$-\left(\frac{G^{n+1}_{j-1}-G^n_{j+1}}{2\Delta\eta}\right)$$

During the even time steps, the calculations started at the last span station outboard and progressed until the root station was reached. The quantity $\hat{G}$ is then modified accordingly and

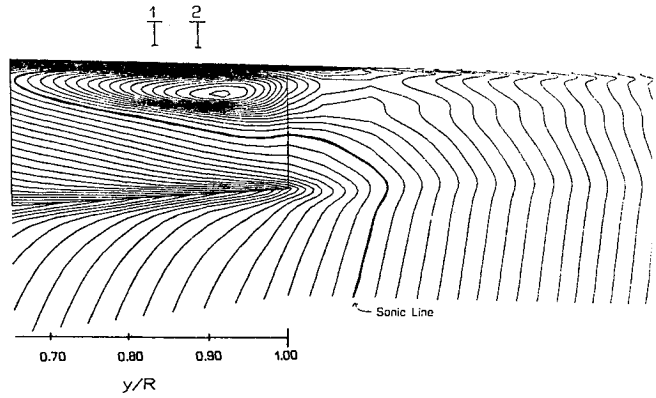

Fig. 2 Mach number contours for a quasisteady ONERA blade. Tip Mach number is 0.6, angle of attack 0.0 deg, advance ratio 0.45, and azimuth angle 90 deg.

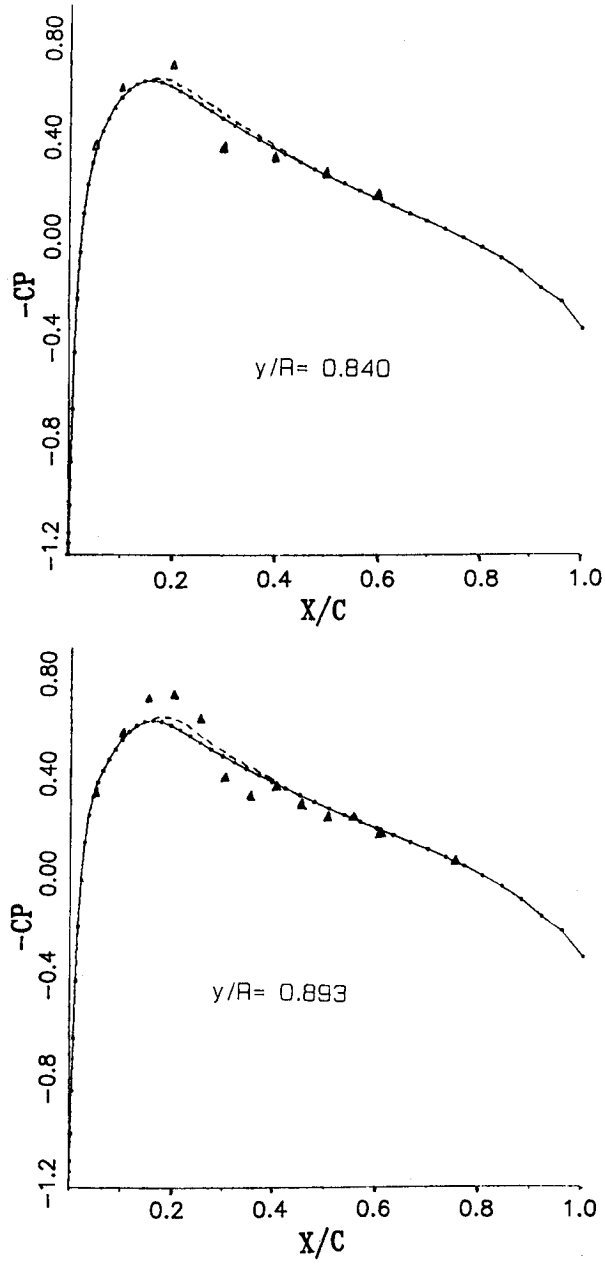

Fig. 3 Pressure distributions at stations indicated in Fig. 2 for the same case. Euler...; Full potential----; Experiment ▲ ▲ ▲.

is written as

$$-\left(\frac{G^{n+1}_{j+1}-G^{n}_{j-1}}{2\Delta\eta}\right)$$

Since this preceding discretization involves a mixture of solution vectors at the n and the $n+1$ time level, the above discretization is a hybird scheme. The reversal of the spanwise direction from one time step to the next removes any dependency that the solution may have on the sweep direction. The above approach has a disadvantage because the spanwise derivatives are no longer conservative with respect to time, although they are conservative with respect to space. With the above discretization, at each of the interior points the following difference equation results for the quantity $\Delta\hat{q}^{n+1}$

$$\left[I+\Delta t\delta_\xi\frac{\partial\hat{E}}{\partial\hat{q}}+\delta_\eta\frac{\partial\hat{H}}{\partial\hat{q}}\right]\Delta\hat{q}^{n+1}=R \tag{9}$$

where for the odd time steps, the residual R is given by

$$R=\frac{-\delta_\xi\hat{F}^n-\delta_\zeta\hat{H}^n-(\hat{G}^n_{j+1}-\hat{G}^{n+1}_{j-1})}{2\Delta\eta} \tag{10}$$

and for the even time steps, the residual is given by

$$R=\frac{-\delta_\xi\hat{F}^n-\delta_\zeta\hat{H}^n-(\hat{G}^{n+1}_{j+1}-\hat{G}^{n}_{j-1})}{2\Delta\eta}$$

If pure central differences are used to discretize the spatial derivatives, it may be shown that an odd-even decoupling of the solution wil occur after only a few time steps. To prevent this, and in order to remove high-frequency errors from the solution, the above finite difference equation was modified, by adding a set of second- and fourth-order dissipation terms and details can be found in Ref. 15.

After the above dissipation terms were added, the left-hand side operator in Eq. (9) was approximately factorized into a

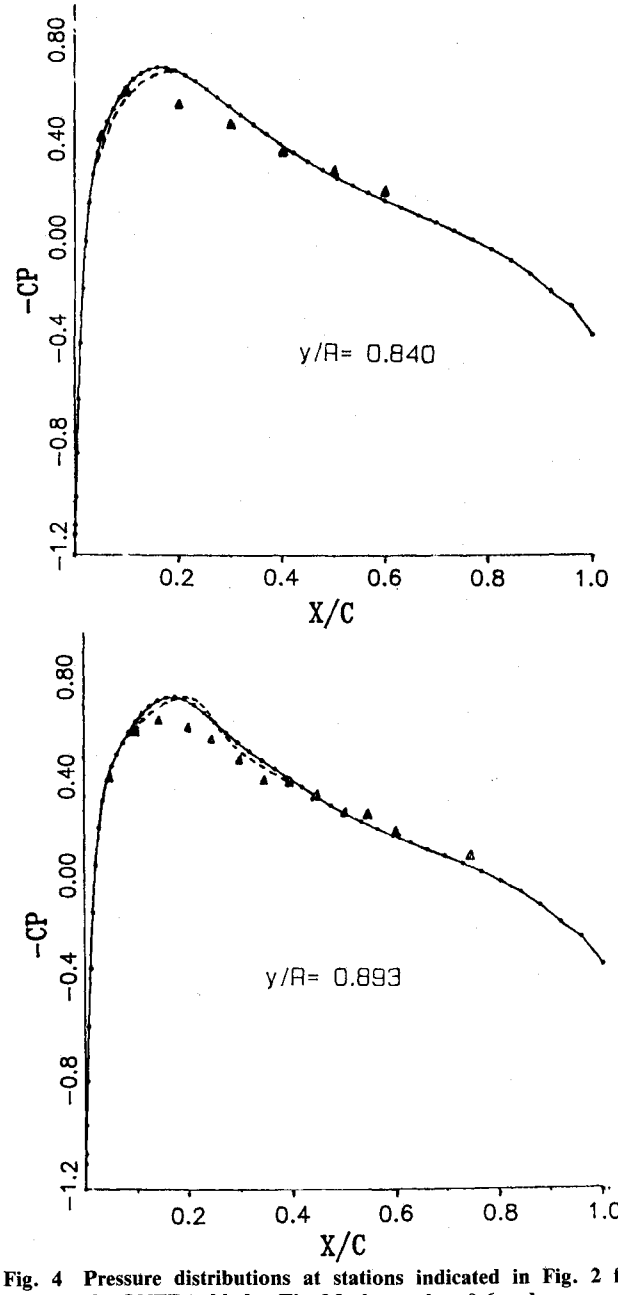

Fig. 4 Pressure distributions at stations indicated in Fig. 2 for quasisteady ONERA blade. Tip Mach number 0.6, advance ratio 0.40, azimuth angle 90 deg. Euler....; Full potential----; Experiment ▲ ▲ ▲.

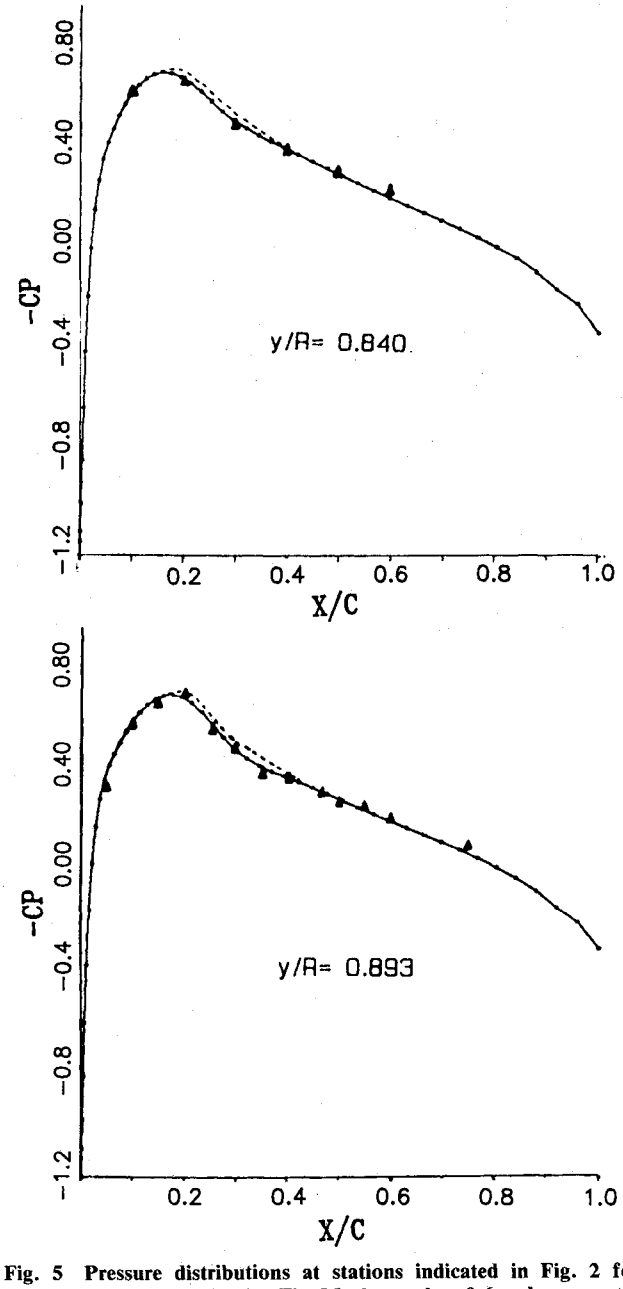

Fig. 5 Pressure distributions at stations indicated in Fig. 2 for quasisteady ONERA blade. Tip Mach number 0.6, advance ratio 0.45, azimuth angle 60 deg. Euler...; Full potential----; Experiment ▲ ▲ ▲.

product of two one-dimensional operators using the Beam-Warming factorization.

This factored equation was solved using a series of block tridiagonal matrix inversions. The values of $\Delta\hat{q}$ at the computational boundaries were set to zero. The flow vector $\hat{q}$ at these boundaries was updated after the interior points were updated.

The way the unsteadiness is generated in this problem is through the motion of the grid. That means that the quantities x_τ, y_τ, z_τ for every grid point are prescribed functions of time. The boundary conditions are as follows.

At every location on the boundaries, with the exception of the left boundary, the direction of the flow is evaluated. For the case of outflow the pressure is set to its undisturbed value and all other quantities are extrapolated from the interior. At the innermost span station, infinite span conditions are used, i.e., all the η-derivatives are set equal to zero and a two-dimensional problem is solved.

In the wake region downstream of the rotor trailing edge, and at the coordinate surface cut beyond the rotor tip, there are two computational points corresponding to a single physical point. The flow properties on these two points were obtained as averages of the flow properties above and below.

At the solid surface, the tangential components of velocity were linearly extrapolated from the interior. The density and pressure values were also extrapolated similarly. For thick rotors with highly curved surfaces, a more accurate means of determining the surface pressure will be through the solution of the normal momentum equation at the wing surface.

The hybrid scheme described here has a number of advantages over existing explicit and implicit time marching procedures. It requires only two tridiagonal block matrix inversions. Conventional alternating-direction implicit schemes require three tridiagonal matrix inversions.

Only one time level of storage is required. That is, only the five flow variables need be stored as three-dimensional arrays. The residuals R and the quantities $\Delta\hat{q}$ may be stored as two-dimensional arrays, since they are used only one span station at a time.

Since the solution vector q is required on only 5 planes at a time, the present procedure may be coded for efficient memory utilization on virtual memory machines such as the CDC Cyber 205 computer.

The quasisteady Euler calculations were all done on a $157\times23\times17$ grid, with 97 points on the airfoil, and 17 span stations on the blade. A partially vectorized version of the Euler solver on a Cyber 205 system required 14.5 s of computer time per time step.

The unsteady Euler calculations were all done on a $121\times16\times21$ grid, with 90 points on the airfoil, and 11 span stations. A completely vectorized version of the Euler solver on a CRAY XMP system required 1.2 s of computer time per time step, and used 800,000 words of memory. A constant value of time step 0.02 was used in these calculations. Since the smallest grid spacing on the sheared parabolic grid was equal to 0.0004 units, this range of time steps corresponds to a CFL number of 100 or more. Use of smaller time steps did not change the results and use of coarser grids led to somewhat smeared shocks.

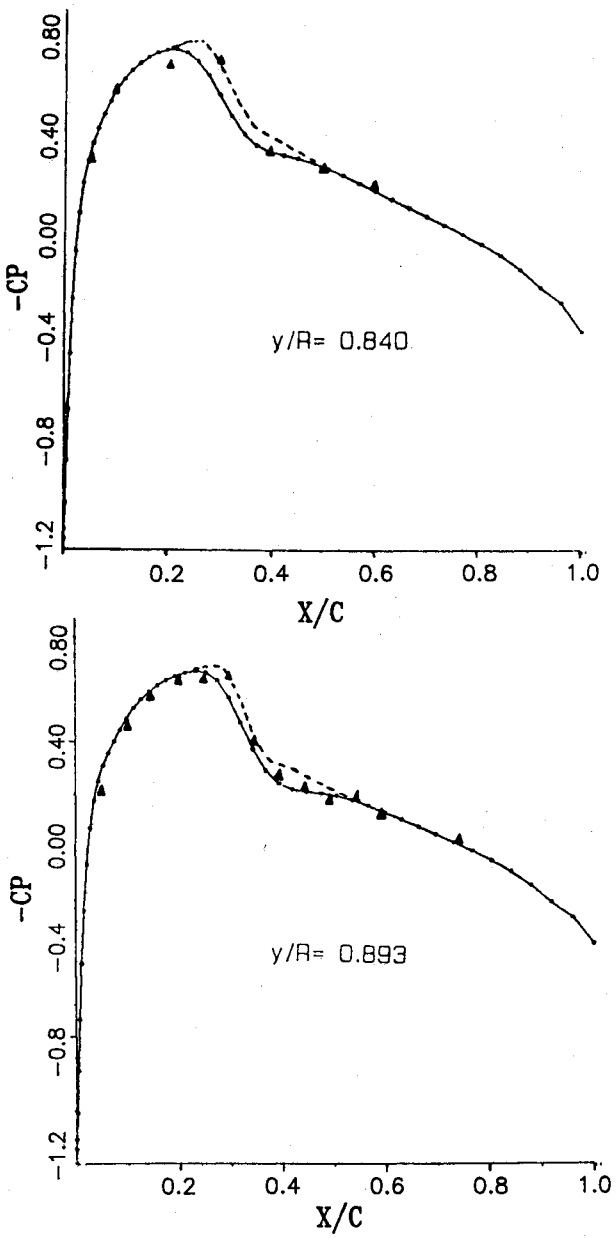

Fig. 6 Pressure distributions at stations indicated in Fig. 2 for quasisteady ONERA blade. Tip Mach number 0.6, advance ratio 0.45, azimuth angle 120 deg. Euler...; Full potential----; Experiment ▲▲▲.

III. Discussion of Results

The numerical algorithm that was discussed in Sec. II of this paper was applied to flows around helicopter blades. Results have been obtained both for steady and unsteady flow cases and are discussed next.

An extensive set of comparisons has been made between Euler results, full potential results, and experimental measurements. The Euler results were obtained by reaching the steady state asymptotically in time after several hundred time steps. Figure 2 shows Mach number contours for the ONERA blade in the blade fixed coordinate system. The sonic line and the formation of the shock are clearly shown. Figures 3-6 show the computed pressure distributions of the ONERA blade at the two stations indicated in Fig. 1. These quasisteady results are compared with experiment and full-potential[7] results for various azimuth locations and two advanced ratios. The agreement between the Euler and full-potential results is excellent for all cases, as it should be. The agreement with experiment is good for most cases as well; the discrepancies that exist may be due to unsteady effects. The excellent agreement between these sets of computations is an indication of the capability of the Euler solver to compute steady transonic flows around rotor blades.

Figures 7 and 8 show, for the first time to the authors' knowledge, unsteady Euler results for a nonlifting rotor, for two advance ratios and several azimuth locations. The computed pressure distributions are compared with the measured data of Ref. 17. The agreement is good for all cases. It should be mentioned that viscous effects are not accounted for in these comparisons.

In conclusion, it can be stated that the Euler solver described in this paper is capable of accurately simulating steady

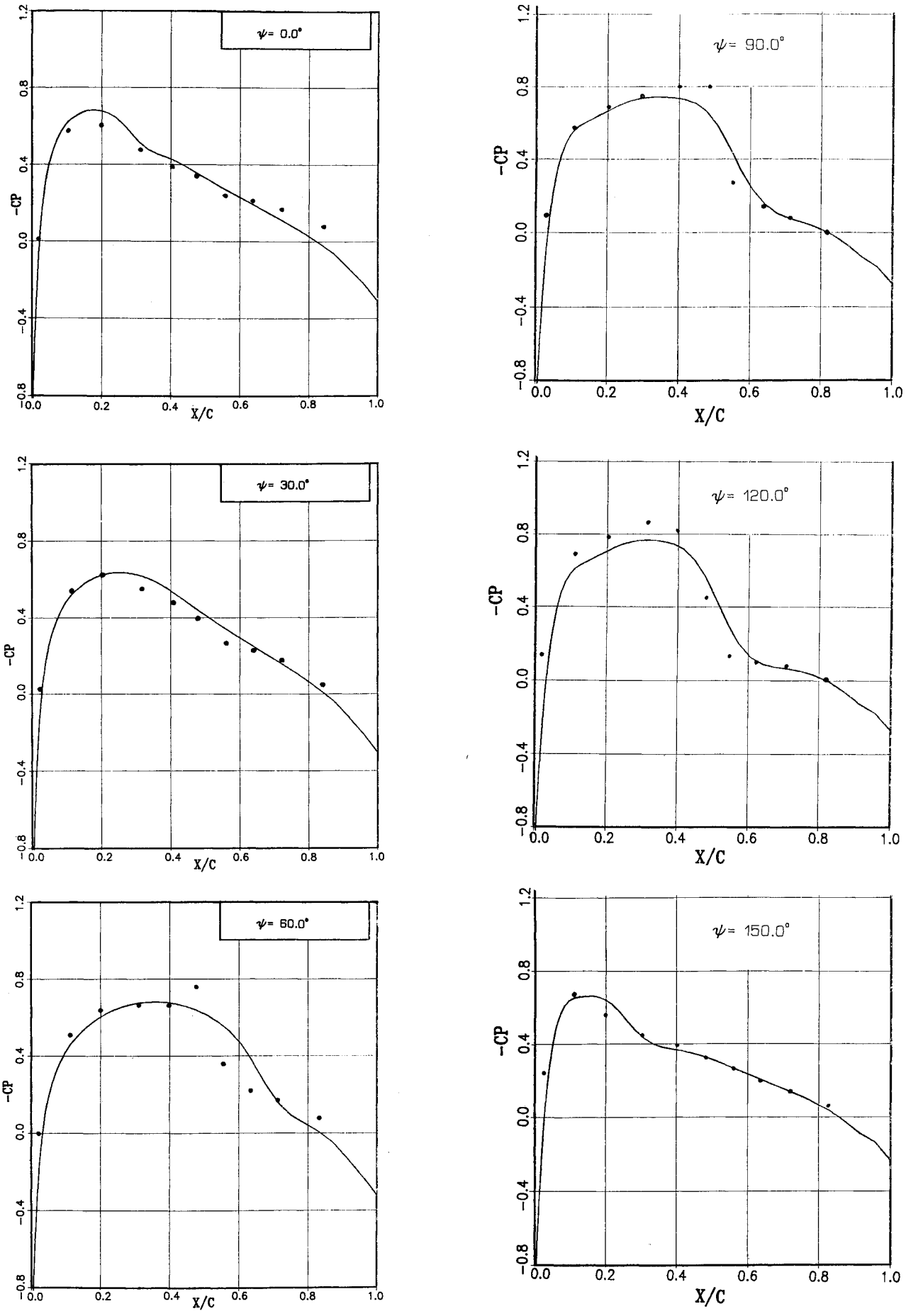

Fig. 7 Pressure distributions for unsteady blade with rectangular planform and NACA 0012 sections. Tip Mach number 0.7, advance ratio 0.3, $y/R = 0.9$. Euler ——; Experiment....

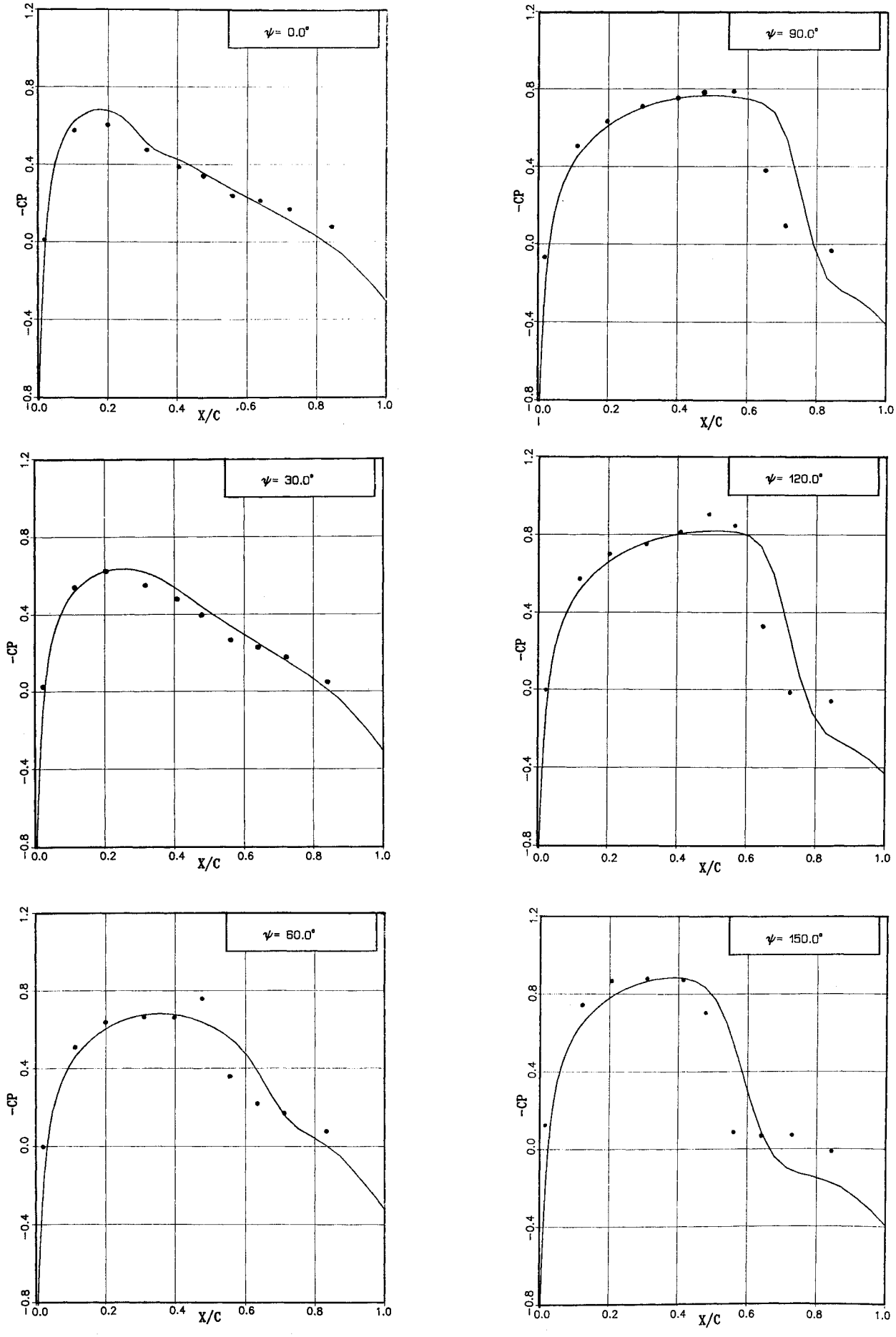

Fig. 8 Pressure distributions for unsteady blade with rectangular planform and NACA 0012 sections. Tip Mach number 0.8, advance ratio 0.2, $y/R = 0.9$. Euler ——; Experiment....

and unsteady transonic flow around nonlifting rotor blades. It should be mentioned that the code has already been coupled with a freewake code and it has been successfully used to obtain lifting results in transonic flow. However, this is the subject of another paper.[18]

Acknowledgment

This work was supported by the Army Research Office under the Center for Rotary Wing Aircraft Technology at the Georgia Institute of Technology. The CDC-205 computer time was provided by the University System of Georgia.

References

[1]Caradonna, F. X. and Isom, M. P., "Subsonic and Transonic Potential Flow Over Helicopter Rotor Blades," *AIAA Journal*, Vol. 10, Dec. 1972, pp. 1606-1612.

[2]Caradonna, F. X. and Isom, M., "Numerical Calculation of Unsteady Transonic Potential Flow Over Helicopter Rotor Blades," *AIAA Journal*, Vol. 14, April 1976, pp. 482-488.

[3]Tung, C., Caradonna, F. X., Boxwell, D. A., and Johnson, W. R., "The Prediction of Transonic Flow on Advancing Rotors," *Proceedings of the 40th Annual National Forum of the American Helicopter Society*, Washington, D. C. 1984.

[4]Caradonna, F. X., Tung, C., and Desopper, A., "Finite-Difference Modelling of Rotor Flows Including Wake Effects," *Journal of the American Helicopter Society*, Vol. 29, April 1984, pp. 26-33.

[5]Arieli, R. and Tauber, M. E., "Computation of Subsonic and Transonic Flow About Lifting Rotor Blades," AIAA Paper 79-1667, 1979.

[6]Tauber, M. E. and Hicks, R. M., "Computerized Three-Dimensional Aerodynamic Design of a Lifting Rotor Blade," *Proceedings of the 36th Annual Forum of the American Helicopter Society*, 1980.

[7]Tauber, M. E., "Computerized Aerodynamic Design of a Transonically 'Quiet-Blade'," *Proceedings of the 40th Annual Forum of the American Helicopter Society*, 1984.

[8]Chang, I. C. and Tung, C., "Numerical Solution of the Full-Potential Equation for Rotors and Oblique-Wings Using a New Wake Model," AIAA Paper 85-0268, 1985.

[9]Egolfe, A. and Sparks, P., "Hover Rotor Airload Predictions Using a Full Potential Flow Analysis with a Realistic Wake Geometry," *Proceedings of the 41st Annual National Forum of the American Helicopter Society*, Ft. Worth, TX, 1985.

[10]Tauber, M. E., Owen, F. K., Langhi, R. G., and Palmer, G. E., "Comparison of Calculated and Measured Velocities Near the Tip of a Model Rotor Blade at Transonic Speeds," NASA TM 86697, 1985.

[11]Chang, I. C., "Transonic Flow Analysis for Rotors Part I and II," NASA TP-2375, 1985.

[12]Tung, C. and Chang, I. C., "Rotor Transonic Computation with Wake Effect," Presented at the Fourth International Conference on Applied Numerical Modeling, Tainan, Taiwan, Dec. 1984.

[13]Sankar, N. L. and Prichard, D., "Solution of Transonic Flow Past Rotor Blades Using the Conservative Full Potential Equation," AIAA Paper 85-5012, 1985.

[14]Roberts, T. W. and Murmann, E. M., "Solution Method for a Hovering Helcopter Rotor Using the Euler Equations," AIAA Paper 85-0436, 1985.

[15]Sankar, N. L., Wake, B. E., and Lekoudis, S. G., "Solution of the Euler Equations for Fixed and Rotor Wing Configurations," *Journal of Aircraft*, Vol. 23, April 1986, pp. 283-289.

[16]Wake, B. E., Sankar, N. L., Lekoudis, S. G., and Gray, R. B., "The Prediction of Flow Around Blade Tips," *Proceedings of the International Conference on Rotorcraft Basic Research*, Research Triangle Park, NC, Feb. 19-21, 1985.

[17]Caradonna, F. X., Laub, G. A., and Tung, C., "An Experimental Investigation of the Parallel Blade-Vortex Interaction" *Proceedings of the Tenth European Rotorcraft Forum*, The Netherlands, Aug. 28-31, 1984.

[18]Sankar, N. L. and Tung, C., "Euler Calculations for Rotor Configurations in Unsteady Forward Flight," *Proceedings of the 42nd Annual Meeting of the American Helicopter Society*, Washington, D.C., 1986.